The Rotational Zeeman Effect of Thiazole and Isothiazole

Jürgen Wiese and Dieter H. Sutter
Abteilung Chemische Physik im Institut für Physikalische Chemie der Universität Kiel

Z. Naturforsch. **35a**, 712–722 (1980); received April 17, 1980

The rotational Zeeman effect of low J rotational transitions ($J \leqq 3$) has been investigated for Thiazole and Isothiazole. The measured susceptibilities are compared to those calculated within the model of localized (atomic) susceptibilities, and nonlocal contributions to the susceptibility component perpendicular to the ring are obtained. These nonlocal susceptibilities, if compared to those of a set of related compounds appear to correlate to the "aromatic character" as determined by chemical reactivity. Five or six membered rings with $\chi_{\perp \text{nonlocal}} < -30 \cdot 10^{-6}$ erg/G^2 mol show "aromatic reactions" while molecules with $-20 \cdot 10^{-6}$ erg/G$^2 < \chi_{\perp \text{nonlocal}}$ show "olefinic reactions".

Introduction

In general aromatic molecules are assumed to be characterized by a ringsystem containing $4n + 2$ more or less delocalized π-electrons [1]. Despite this appearently well defined basic property of aromatic molecules, it is not easy to define aromaticity in a unique way in terms of measurable physical or chemical quantities [2]. One method proposed to "measure" aromaticity is to investigate the diamagnetic susceptibility perpendicular to the ring whose nonlocal contribution is related to the nonlocal (molecular) diamagnetic ring current and thus – at least intuitively – to the delocalisation of the π-system [3]. In principle the nonlocal susceptibility should be extractable from NMR-shielding/deshielding data, but strong local contributions may considerably complicate the analysis [4]. In the case of rotational Zeeman spectroscopy, where the molecular susceptibility anisotropies of free molecules are measured directly, such complications do not arise. In the following we report the results of a rotational Zeeman effect study for Thiazole and Isothiazole which closes a gap in the system of five membered rings studied so far [5]. This enables us to give a better judgement of the use of the nonlocal susceptibility perpendicular to the ring [6] as a measure for "aromaticity".

Experimental

P.a. grade Thiazole and Isothiazole from Merck, Germany, were used after a bulb to bulb destillation without further purification. The spectra were recorded with a conventional Stark-effect modulated microwave spectrometer using 33 kHz square wave modulation. For the Zeeman measurements the spectrometer is equipped with an electromagnet capable to deliver a field of about 25 kG (2.5 Tesla) over a gap of 3.5 cm height and 2.5 m length. Details of the spectrometer may be found in Ref. [5 b] and [7]. Under typical recording conditions sample pressures were about 5 m Torr ($7 \cdot 10^{-6}$ Pascal) and cell temperatures were about -50 °C. At these conditions zero field linewidths (half width at half height) of 80 to 100 kHz were obtained and the ^{14}N quadrupole hyperfine structure was generally well resolved. With the magnetic field set to about 25 kG the absorption lines further split with overall splittings on the order of 1 to 6 MHz depending on the rotational transition under investigation. Since the presence of the ^{14}N quadrupole nucleus with spin $I = 1$ triples the number of Zeeman satellites as compared to the standard rigid rotor case, overlapping of lines frequently occurs in the Zeeman patterns. It was however possible to arrive at a unique assignment of the recorded Zeeman statellites and to determine accurate molecular g-values and susceptibility anisotropies for both molecules.

Analysis of the Spectra

The molecular parameters for the Thiazoles were determined in a two step procedure. In the first step the rotational constants and ^{14}N nuclear quadrupole coupling constants were fitted to the zero field spectra (Tables 1 and 2). Since only rotational transitions with $J \leqq 3$ were used, centrifugal distortions proved negligible and the spectra could be

---

Reprint requests to Prof. Dr. D. H. Sutter, Institut für Physikalische Chemie, Universität Kiel Abt. Chemische Physik, Olshausenstr. 40–60, D-2300 Kiel.

0340-4811 / 80 / 0700-0712 $ 01.00/0. — Please order a reprint rather than making your own copy.

Table 1. Observed and deviations to calculated frequencies of rotational transitions of Thiazole and Isothiazole. The calculated frequencies were determined by using the model of the rigid rotor. The observed frequencies are averages of the measured hyperfine transition frequencies corrected by the calculated hyperfine splitting (using the constants of Table 4).

Transition	Thiazole		Isothiazole	
$J_{K_-K_+} \to J'_{K'_-K'_+}$	ν_{exp}/MHz	$\Delta\nu_{e-c}$/kHz	ν_{exp}/MHz	$\Delta\nu_{e-c}$/kHz
$0_{00} \to 1_{01}$	8 850.087	34	9 270.479	58
$0_{00} \to 1_{11}$	11 873.747	24	11 699.791	23
$1_{01} \to 2_{12}$	18 562.318	− 2	18 548.181	26
$1_{11} \to 2_{02}$	13 863.047	11	14 989.413	32
$1_{11} \to 2_{12}$	15 538.678	29	—	
$1_{11} \to 2_{20}$	31 907.469	41	31 795.085	20
$1_{10} \to 2_{11}$	19 861.580	18	20 962.896	20
$1_{10} \to 2_{21}$	28 932.553	−19	28 250.913	− 4
$2_{02} \to 2_{11}$	8 160.017	35	8 395.531	−18
$2_{12} \to 2_{21}$	15 555.362	−17	14 554.139	− 5
$2_{11} \to 2_{20}$	9 884.396	−13	8 410.137	−18
$2_{02} \to 3_{03}$	—		24 339.652	5
$2_{12} \to 3_{13}$	22 867.347	4	23 583.406	7
$2_{11} \to 3_{12}$	29 143.435	−27	30 480.288	−61
$2_{21} \to 3_{22}$	26 550.157	− 2	27 811.234	−29
$2_{20} \to 3_{21}$	29 252.375	−39	31 282.866	−13
$2_{11} \to 3_{22}$	35 621.161	− 8	—	
$3_{13} \to 3_{12}$	—		14 163.069	17

Table 2a. Observed and calculated frequencies of hyperfine transitions of Thiazole used for fitting the nuclear quadrupole coupling constants (s. Table 4). If overlapping of lines occurs the intensity weighted averages of the calculated frequencies are given.

$J_{K_-K_+} \to J'_{K'_-K'_+}$	F	F'	ν_{exp}/MHz	$\Delta\nu_{exp}$/kHz	$\Delta\nu_{calc}$/kHz
$0_{00} \to 1_{01}$	1	2	8 850.217	817.00	813.00
	1	1	8 849.400		
	1	2	8 850.217	−1238.00	−1218.00*
	1	0	8 851.455		
$1_{01} \to 2_{12}$	2	3	18 562.382	798.00	782.00
	1	2			
	0	1	18 561.584		
	2	2			
$1_{11} \to 2_{02}$	2	3	13 863.286	1027.00	1008.00
	1	2	13 862.259		
	2	3	13 863.286	− 564.00	− 598.00
	0	1	13 863.850		
$1_{11} \to 2_{12}$	2	3	15 538.865	825.00	860.00
	1	2	15 538.040		
	2	2			
$1_{11} \to 2_{20}$	2	3	31 907.281	557.00	495.00
	0	1	31 906.724		
	2	3	31 907.281	− 940.00	− 958.00
	1	2	31 908.221		
$1_{10} \to 2_{11}$	1	2	19 860.906	− 808.00	− 816.00
	2	3	19 861.714		
$1_{10} \to 2_{21}$	0	1	28 933.129	1896.00	1946.00
	1	1	28 931.233		
$2_{02} \to 2_{11}$	3	3	8 159.792	519.00	526.00
	1	1	8 159.273		
	3	3	8 159.792	− 986.00	− 947.00
	2	2	8 160.778		
$2_{12} \to 2_{21}$	3	3	15 554.984	−1708.00	−1705.00
	2	2	15 556.692		
	3	3	15 554.984	961.00	947.00
	1	1	15 554.023		
	3	3	15 554.984	− 383.00	− 378.00
	2	1	15 554.367		
	1	2			

* In Tables 2 and 3 the two zeros trailing the decimal point have no meaning. Experimental satellite frequency uncertainties are ± 5 kHz for well resolved lines and ± 10 kHz to ± 20 kHz for peak frequencies originating from overlapping lines. The calculated frequencies have been rounded to the next full kHz value.

Table 2a. (continued 1).

$J_{K_-K_+} \rightarrow J'_{K'_-K'_+}$	$F \rightarrow F'$	ν_{exp}/MHz	$\Delta\nu_{\text{exp}}$/kHz	$\Delta\nu_{\text{calc}}$/kHz
$2_{21} \rightarrow 3_{22}$	3 4	26 550.351	871.00	870.00
	3 3			
	2 3	26 549.480		
	2 2			
	3 4	26 550.351	−481.00	−484.00
	3 3			
	1 2	26 550.832		
$2_{20} \rightarrow 3_{21}$	3 4	29 252.548	750.00	738.00
	2 3	29 251.798		
	3 4	29 252.548	−424.00	−460.00
	1 2	29 252.972		
$3_{30} \rightarrow 4_{31}$	4 5	37 697.643	729.00	720.00
	3 4	37 696.914		

Table 2b. Observed and calculated frequencies of some hyperfine transitions of Isothiazole used for fitting the nuclear quadrupole coupling constants (s. Table 4). If overlapping of lines occurs the intensity weighted averages of the calculated frequencies are given.

$J_{K_-K_+} \rightarrow J'_{K'_-K'_+}$	$F \rightarrow F'$	ν_{exp}/MHz	$\Delta\nu_{\text{exp}}$/kHz	$\Delta\nu_{\text{calc}}$/kHz
$0_{00} \rightarrow 1_{11}$	1 2	11 699.909	704.00	722.00
	1 1	11 699.205		
	1 2	11 699.909	−1068.00	−1082.00
	0 1	11 700 977		
$1_{01} \rightarrow 2_{12}$	1 2	18 547.589	−731.00	−751.00
	2 3	18 548.320		
	1 2	18 547.589	−1448.00	−1461.00
	0 1	18 549.037		
$1_{11} \rightarrow 2_{02}$	2 3	14 989.962	−656.00	−662.00
	1 2	14 989.306		
$1_{11} \rightarrow 2_{20}$	2 3	31 794.962	1151.00	1115.00
	0 1	31 793.811		
	2 3	31 794.962	−759.00	−781.00
	1 2	31 795.721		
$1_{10} \rightarrow 2_{21}$	2 3	28 251.054	741.00	744.00
	1 2	28 250.313		
	2 3	28 251.054	−819.00	−800.00
	0 1	28 251.873		
$2_{02} \rightarrow 2_{11}$	3 3	8 395.364	−799.00	−833.00
	2 2	8 396.163		
$2_{11} \rightarrow 3_{22}$	3 4	35 099.455	794.00	773.00
	2 3	35 098.661		
	3 4	35 099.455	−418.00	−430.00
	1 2	35 099.873		
$2_{21} \rightarrow 3_{22}$	2 3	27 811.500	351.00	334.00
	3 4	27 811.149		
$2_{20} \rightarrow 3_{21}$	1 2	31 282.492	−868.00	−863.00
	2 3	31 283.360		
	1 2	31 282.492	−198.00	−215.00
	3 4	31 282.690		
$3_{13} \rightarrow 3_{12}$	4 4	14 162.786	−1176.00	−1146.00
	3 3	14 163.944		

fitted to the standard rigid rotor energy expression [8]. Only the quadrupole coupling matrix elements diagonal in J (and I) are included in this energy expression. This approximation holds very good in the case of the weakly coupled ^{14}N nucleus. It is however insufficient to reproduce the microwave spectra of molecules containing strongly coupled nuclei such as for instance ^{81}Br.

In the second step the molecular g-values and susceptibility anisotropies were fitted to the high-field Zeeman hyperfine patterns (Tables 3 a and 3 b). For this fit the rotational constants and quadrupole coupling constants were kept fixed to their values derived from the zero field spectra (Table 4). Again hyperfine- (and Zeeman-) matrix elements off diagonal in the rotational quantum numbers J and $K_- K_+$ were neglected. For each rotational state the corresponding $M_J M_I$ submatrix was set up in the uncoupled basis $|J, K_- K_+, M_J\rangle |I, M_I\rangle$ [9] and sufficiently accurate sublevel energies were calculated by second order perturbation theory. This considerably simplifies the least squares procedure. A posteriori the validity of this second order perturbation treatment was checked by diagonalizing the submatrices for each rotational state numerically. The Zeeman-hyperfine-splittings

Table 3a. Observed and calculated frequency splittings of some Zeeman-hyperfine-satellites of Thiazole with respect to the corresponding hypothetical rigid rotor frequencies. The given splittings were used to fit the Zeeman parameters (see Table 5). Since the magnetic field effectively uncouples overall and spin angular momentum, M_J and M_I rather than M_F and F are the appropriate quantum numbers to label the rotational states with $\Delta M_I = 0$ as selection rule for the ^{14}N spin. If overlapping of lines occurs, the calculated splittings are intensity averaged splittings (see text).

Transition $J_{K_-K_+} \to J'_{K'_-K'_+}$	$M_J \to$	M_J	M_I	$\Delta\nu_{\mathrm{exp}}$/kHz	$\Delta\nu_{\mathrm{calc}}$/kHz
$0_{00} \to 1_{01}$	0	0	−1	−831.00	−832.00
25.62 kGauss	0	0	1		
	0	0	0	−22.00	−19.00
$0_{00} \to 1_{01}$	0	−1	0	−476.00	−466.00
19.75 kGauss	0	−1	−1	−70.00	−80.00
	0	−1	1		
	0	1	0	226.00	254.00
	0	1	−1	662.00	675.00
	0	1	1		
$0_{00} \to 1_{11}$	0	0	−1	−569.00	−556.00
25.62 kGauss	0	0	0		
	0	0	1		
$0_{00} \to 1_{11}$	0	−1	−1	−316.00	−327.00
19.75 kGauss	0	−1	0		
	0	−1	1		
	0	1	−1	657.00	658.00
	0	1	0		
	0	1	1		
$1_{11} \to 2_{20}$	−1	−1	−1	−975.00	−965.00
25.62 kGauss	−1	−1	1		
	0	0	−1	1361.00	1360.00
	1	1	−1		
	0	0	1		
	1	1	1		
$1_{10} \to 2_{11}$	0	0	−1	−967.00	−986.00
25.62 kGauss	0	0	1		
	0	0	0	−87.00	−128.00
	1	1	0		
	1	1	−1	294.00	315.00
	1	1	1		
	−1	−1	−1	1463.00	1450.00
	−1	−1	1		
$1_{10} \to 2_{11}$	0	−1	−1	−2312.00	−2326.00
24.21 kGauss	0	−1	1		
	0	−1	0	−1519.00	−1533.00
	1	0	−1	−813.00	−837.00
	−1	−2	0		
	1	0	1		
	−1	−2	−1	−437.00	−423.00
	−1	−2	1		
	0	1	−1	168.00	161.00
	0	1	1		
	1	2	0	606.00	579.00
	1	2	−1	985.00	980.00
	0	1	0		
	1	2	1		

Table 3a (continued 1).

Transition $J_{K_-K_+} \rightarrow J'_{K'_-K'_+}$	$M_J \rightarrow M_J'$	M_I	$\Delta\nu_{\text{exp}}$/kHz	$\Delta\nu_{\text{calc}}$/kHz
$2_{02} \rightarrow 2_{11}$ 25.62 kGauss	−2 −2	−1	−3490.00	−3486.00
	−2 −2	1		
	−2 −2	0	−2850.00	−2851.00
	2 2	−1	946.00	972.00
	2 2	1		
	2 2	0	1581.00	1598.00
$2_{02} \rightarrow 2_{11}$ 19.75 kGauss	−1 −2	−1	−1811.00	−1805.00
	−1 −2	1		
	−2 −1	−1	−1127.00	−1077.00
	0 −1	0		
	−2 −1	1		
	0 −1	−1	− 303.00	− 297.00
	0 −1	1		
	1 0	−1	332.00	343.00
	−1 0	0		
	1 0	1		
	2 1	1		
	0 1	−1	1703.00	1706.00
	1 2	0		
	0 1	1		
$2_{11} \rightarrow 2_{20}$ 19.75 kGauss	−1 −2	−1	−2456.00	−2448.00
	−1 −2	1		
	0 −1	−1	−1252.00	−1252.00
	1 0	0		
	0 −1	1		
	1 0	−1	− 510.00	− 510.00
	2 1	0		
	1 0	1		
	1 2	−1	1016.00	1031.00
	1 2	1		
	0 1	0		
	−1 0	−1	1469.00	1471.00
	0 1	−1		
	−1 0	1		
	0 1	1		
$2_{12} \rightarrow 3_{13}$ 21.98 kGauss	1 0	−1	− 561.00	− 582.00
	1 0	1		
	−1 0	−1		
	2 3	0	− 410.00	− 382.00
	−1 0	1		
	0 1	−1	− 10.00	− 42.00
	2 3	−1		
	−1 0	0		
	0 1	0		
	0 1	1		

calculated by the two methods differ by 5 kHz at most, which is still within the experimental uncertainty of the frequency determinations and thus justifies the use of the second order perturbation treatment. If – as was frequently the case – two or even more Zeeman hyperfine satellites overlapped within one zerofield halfwidth, the observed peak frequency was assumed to be sufficiently well reproduced by the intensity weighted average frequency of the constituent satellites (compare Ref. [10] for a detailed discussion of the analysis of unresolved lines). The diagonal elements of the molecular g-tensor and the anisotropies of the magnetic susceptibility tensor obtained by the least squares fit to the splittings are given in Table 5. Also listed in Table 5 are the molecular electric quadrupole moments, the individual components of the diagonal elements of the susceptibility tensor, and the ground state expectation values for the sums of the squares of the electron coordinates, all referred to the principial axis systems of the moment of inertia tensor (center of mass system). To

Table 3b. Observed and calculated frequency splittings of some Zeeman-hyperfine-satellites of Isothiazole.

Transition $J_{K_-K_+} \rightarrow J'_{K'_-K'_+}$	$M_J \rightarrow M_J'$	M_I	$\Delta\nu_{\text{exp}}$/kHz	$\Delta\nu_{\text{calc}}$/kHz
$0_{00} \rightarrow 1_{01}$	0 −1	−1	− 142.00	− 142.00
19.75 kGauss	0 1	1		
	0 −1	−1	388.00	400.00
	0 1	1		
$0_{00} \rightarrow 1_{11}$	0 0	−1	− 766.00	− 799.00
25.62 kGauss	0 0	1		
$0_{00} \rightarrow 1_{11}$	0 −1	−1	− 404.00	− 386.00
19.75 kGauss	0 −1	1		
	0 1	−1	942.00	959.00
	0 1	1		
$1_{11} \rightarrow 2_{20}$	−1 −1	−1	−1187.00	−1208.00
25.63 kGauss	−1 −1	1		
	−1 −1	0	− 875.00	− 872.00
	0 0	0	805.00	783.00
	1 1	−1	1171.00	1153.00
	1 1	1		
	0 0	−1	1526.00	1534.00
	1 1	0		
	0 0	1		
$1_{11} \rightarrow 2_{20}$	−1 −2	−1	−4036.00	−4074.00
24.21 kGauss	−1 −2	1		
	−1 −2	0	−3680.00	−3680.00
	0 −1	0	−1568.00	−1594.00
	0 −1	−1	− 835.00	− 852.00
	0 −1	1		
	1 0	−1	− 512.00	− 515.00
	1 0	1		
	1 2	−1	2049.00	2000.00
	1 2	1		
	0 1	0	2364.00	2358.00
	1 2	0		
	0 1	−1	3024.00	2997.00
	0 1	1		
$1_{10} \rightarrow 2_{11}$	0 0	−1	− 753.00	− 769.00
25.63 kGauss	0 0	0		
	0 0	1		
	1 1	0	− 270.00	− 264.00
	1 1	−1	211.00	209.00
	1 1	1		
	−1 −1	0	1229.00	1215.00
	−1 −1	−1	1668.00	1666.00
	−1 −1	1		
$1_{10} \rightarrow 2_{21}$	−1 −1	−1	1011.00	935.00
24.11 kGauss	−1 −1	0		
	−1 −1	1		
$1_{10} \rightarrow 2_{21}$	0 −1	−1	−2733.00	−2713.00
24.21 kGauss	0 −1	1		
	0 −1	0	−2202.00	−2191.00
	−1 −2	0	−1617.00	−1622.00
	−1 −2	−1	−1159.00	−1191.00
	−1 −2	1		
	0 1	−1	677.00	671.00
	0 1	1		
	0 1	0	1271.00	1274.00
	1 2	0		
	1 2	−1	1734.00	1741.00
	1 2	1		
	−1 0	−1	2823.00	2827.00
	−1 0	0		
	−1 0	1		

Table 3b (continued 1).

Transition $J_{K_-K_+} \rightarrow J'_{K'_-K'_+}$	$M_J \rightarrow M_J'$	M_I	$\Delta\nu_{\text{exp}}$/kHz	$\Delta\nu_{\text{calc}}$/kHz
$2_{02} \rightarrow 2_{11}$ 19.75 kGauss	−1 −2	−1	−2098.00	−2128.00
	−1 −2	1		
	−2 −1	−1	−1063.00	−1098.00
	−2 −1	1		
	0 −1	−1	− 325.00	− 351.00
	0 −1	1		
	0 1	−1	1717.00	1699.00
	1 2	−1		
	0 1	1		
	1 2	1		
$2_{12} \rightarrow 2_{21}$ 25.63 kGauss	−2 −2	−1	−4617.00	−4627.00
	−2 −2	0		
	−2 −2	1		
	−1 −1	−1	−1047.00	−1047.00
	−1 −1	0		
	−1 −1	1		
	2 2	−1	2124.00	2089.00
	2 2	0		
	2 2	1		
$2_{11} \rightarrow 2_{20}$ 25.62 kGauss	−2 −2	−1	−1611.00	−1636.00
	−2 −2	1		
	−1 −1	−1	− 621.00	− 648.00
	−1 −1	1		
	1 1	−1	877.00	813.00
	2 2	0		
	1 1	1		
	2 2	−1	1234.00	1286.00
	2 2	1		
$2_{11} \rightarrow 2_{20}$ 19.75 kGauss	0 −1	−1	−1750.00	−1753.00
	0 −1	1		
	1 0	−1	− 784.00	− 760.00
	1 0	1		
	2 1	−1	205.00	182.00
	2 1	1		
	−2 −1	0	543.00	553.00
$2_{20} \rightarrow 3_{21}$ 25.63 kGauss	1 1	−1	− 308.00	− 366.00
	2 2	−1		
	0 0	0		
	2 2	0		
	1 1	1		
	2 2	1		
	−1 −1	0	334.00	325.00
	−1 −1	−1	610.00	617.00
	−1 −1	1		
	−2 −2	−1	1730.00	1739.00
	−2 −2	0		
	−2 −2	1		

calculate the quadrupole moments the structures given in Fig. 1 were used. To calculate the individual components of the susceptibilities the liquid phase bulk susceptibility of Thiazole [11] was used as additional information. Since liquid phase and gasphase susceptibilities may differ, we increased the uncertainty limits of the bulk value to $\pm 2 \cdot 10^{-6}$ erg/G^2 mol for Thiazole and to $\pm 3 \cdot 10^{-6}$ erg/G^2 mol for Isothiazole as compared to $\pm 0.5 \cdot 10^{-6}$ erg/G^2 mol which to our experience is a typical experimental uncertainty for a liquid phase bulk susceptibility determination using the Faraday method [12] or an NMR technique [13]. For a discussion of the implicit neglect of molecular vibra-

Table 4. Rotational constants and nuclear quadrupole coupling constants, $\chi^{N^{14}}$, of Thiazole and Isothiazole (see Table 1 and 2). Our values agree within two standard deviations with those of the earlier determinations[18,19]. However our values for Isothiazole could be determined with experimental uncertainties reduced by a factor of 20 as comparedto the earlier investigation [18].

	Thiazole	Isothiazole
A/MHz	8529.425 (4)	8275.575 (5)
B/MHz	5505.755 (3)	5846.228 (3)
C/MHz	3344.298 (3)	3424.193 (3)
$\chi_{aa}^{N^{14}}$/MHz	− 2.708 (22)	1.037 (23)
$\chi_{bb}^{N^{14}}$/MHz	0.113 (34)	− 2.404 (27)
$\chi_{cc}^{N^{14}}$/MHz	2.595 (34)	1.367 (27)

tions in the evaluation of the molecular quadrupole moments the reader is referred to Ref. [5 b], Chapter II B.

Local and Nonlocal Susceptibilities

Pascal [14] was the first to introduce the concept of local susceptibilities to calculate bulk susceptibilities from atomic increments. When the more detailed information obtained from rotational Zeeman effect measurements on free molecules became available, Benson and Flygare [15] developed a scheme to calculate the individual components of the molecular susceptibility tensors from atomic tensors as building blocks [16]. The orientation of the atomic susceptibility tensors with respect to the molecular frame is determined by the orientation of the bond directions and a rough allowance for the special bonding situation of the atom under consideration is made by assigning different atomic susceptibility tensors to say sp²- and sp³-hybridized carbon atoms etc. Since the first table of local

Table 5. Molecular quantities derived from the experimental data given in Tables 3, the geometries of the nuclear frames and the bulk magnetic susceptibilities. Quoted uncertainties are standard errors of the least squares fit.

		Thiazol	Isothiazol
Molecular g-values	g_{aa}	− 0.1057 (3)	− 0.1287 (3)
	g_{bb}	− 0.0847 (3)	− 0.0785 (3)
	g_{cc}	0.0404 (3)	0.0433 (3)
Molar magnetic susceptibility anisotropies	$N_L(2\chi_{aa}-\chi_{bb}-\chi_{cc})$ [10^{-6} erg/(G² mole)]	51.3 (5)	55.5 (6)
	$N_L(2\chi_{bb}-\chi_{cc}-\chi_{aa})$ [10^{-6} erg/(G² mole)]	50.7 (5)	51.0 (6)
Liquid phase bulk magnetic susceptibilities in units of 10^{-6} erg/(G² mole)	χ_{bulk}	−50.6 (20)	−50.6 (30)
Molecular quadrupole moments in units of 10^{-26} esu cm²	Q_{aa}	− 3.2 (5)	5.1 (6)
$Q_{aa}=\frac{\lvert e\rvert}{2}\left\{\sum_n^{\text{nuclei}} Z_n(2a_n^2-b_n^2-c_n^2)-\langle 0\rvert\sum_s^{\text{electrons}}(2a_\varepsilon^2-b_\varepsilon^2-c_\varepsilon^2)\lvert 0\rangle\right\}$	Q_{bb}	8.0 (6)	0.0 (6)
$=-\frac{h\lvert e\rvert}{16\pi^2 M_p}\left\{\frac{2g_{aa}}{A}-\frac{g_{bb}}{B}-\frac{g_{cc}}{C}\right\}-\frac{2mc^2}{\lvert e\rvert}\{2\chi_{aa}-\chi_{bb}-\chi_{cc}\}$	Q_{cc}	− 4.8 (9)	− 5.1 (10)
Magnetic susceptibilities in units of 10^{-6} erg/(G² mole)	χ_{aa}	−33.5 (22)	−32.1 (32)
	χ_{bb}	−33.7 (22)	−33.6 (32)
	χ_{cc}	−84.6 (23)	−86.1 (34)
Second moments of the nuclear charge distribution calculated from the geometry of the nuclear frame given in Å²	$\sum_n Z_n a_n^2$	48.2 (1)	47.8 (5)
	$\sum_n Z_n b_n^2$	35.4 (1)	34.7 (5)
	$\sum_n Z_n c_n^2$	0.0 (0)	0.0 (0)
Second moments of the electronic charge distribution in Å²	$\langle 0\rvert\sum_\varepsilon a_\varepsilon^2\lvert 0\rangle$	55.9 (10)	54.4 (22)
$\left\langle 0\rvert\sum_l^{\text{electrons}} a_\varepsilon^2\lvert 0\right\rangle=-\frac{2mc^2}{e^2}(\chi_{bb}+\chi_{cc}-\chi_{aa})$	$\langle 0\rvert\sum_\varepsilon b_\varepsilon^2\lvert 0\rangle$	41.5 (10)	42.0 (22)
$-\frac{h}{16\pi^2 m_p}\left(\frac{g_{bb}}{B}+\frac{g_{cc}}{C}-\frac{g_{aa}}{A}\right)+\sum_n^{\text{nuclei}} Z_n a_n^2$	$\langle 0\rvert\sum_\varepsilon c_\varepsilon^2\lvert 0\rangle$	7.9 (10)	8.0 (22)

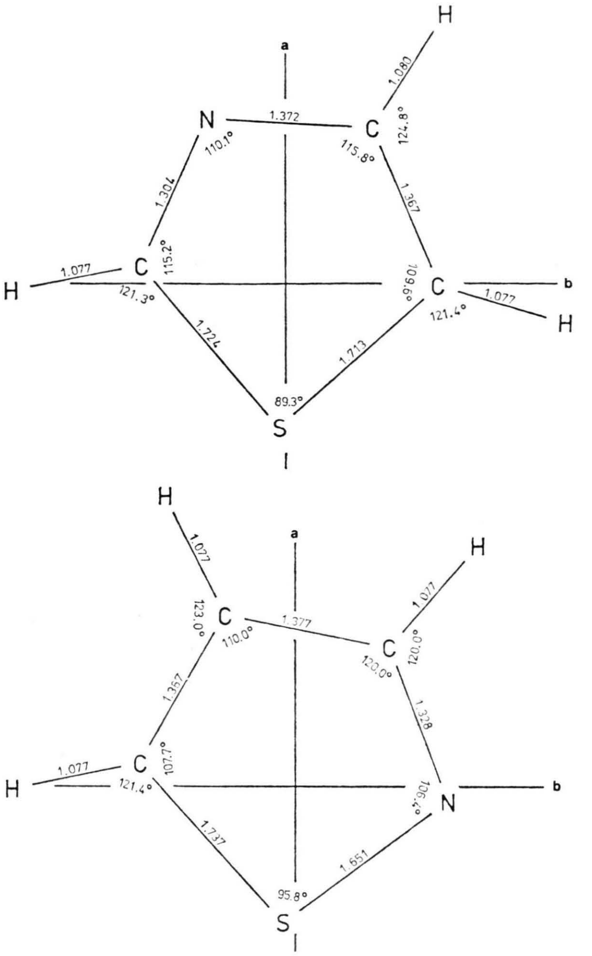

Fig. 1. Structures and orientation of the principal inertia axes system of Thiazole and Isothiazole used to calculate the molecular electric quadrupole moments etc. from the Zeeman data. While the given structure of Thiazole is a r_S-structure, determined by the substituation method from the rotational constants of an extensive set of isotopes [19], the given structure for Isothiazole is only an estimated structure, based on the discussion given in Ref. [20] and in accordance with the observed rotational constants (Table 4).

Table 6. Increments of the local atomicmagne tic susceptibility components used for the calculations of χ_{local} (see Table 7). The increments are given in units of 10^{-6} erg/G^{2}mol.

$\uparrow y$ $\longrightarrow x$ Atom	$\chi_\parallel$	$\chi_\perp$
H–	– 1.70	– 2.11
C=	– 3.54	– 7.11
O=	0.15	– 5.86
O<	– 9.43	– 8.20
S<	–17.0	–14.8
N< (planar)	–11.9	– 6.1
N=	0.	– 4.
F–	– 7.6	– 5.6

susceptibilities was presented by Schmalz, Norris and Flygare [17], the available data has increased considerably and a revised and extended table of local susceptibilities was published in 1976 [5 b]. In Table 6 we give that part of our present list of local susceptibilities which was used for the subsequent discussion. As already shown in the earlier publications, the model of local susceptibilities described above appears indeed well suited to predict the molecular susceptibility tensor in molecules with localized bonds. It is also well suited to predict the average in-plane susceptibility in aromatic rings. It fails however completely to reproduce the susceptibility component perpendicular to the plane of the aromatic rings which generally turns out to be more negative than predicted within the local model. Intuitively this excess "nonlocal" susceptibility may be attributed to an aromatic field induced ring current, a concept commonly used in NMR spectroscopy.

To demonstrate the presence of the nonlocal (ring current) contribution in aromatic molecules, we list the experimental and calculated susceptibilities for a number of five- and six membered rings in Table 7. Isoprene, included at the top of the table, is intended as an example of a nonaromatic molecule in which quite generally both, the average in plane and the out of plane susceptibility are reasonably well reproduced by the local model.

As is seen from the table, the closely related molecules Thiazole, Isothiazole and Thiophene as well as Oxazole, Isoxazole and Furane show almost identical values for $\chi_\perp^{\text{nonlocal}}$. The same holds for the group of benzene derivatives and Pyridine.

In such a group the molecules show great similarities in their chemical reactions and it appears that a correlation exists between $\chi_\perp^{\text{nonlocal}}$ and chemical behaviour. Molecules with $\chi_\perp^{\text{nonlocal}} < -30 \cdot 10^{-6}$ erg/G^2 mol show typical aromatic reactions but no olefinic reactions. Molecules with $\chi_\perp^{\text{nonlocal}} > -20 \cdot 10^{-6}$ erg/G^2 mol only show olefinic reactions and molecules with $\chi_\perp^{\text{nonlocal}} \sim -25 \cdot 10^{-6}$ erg/G^2 mol show both types of reactions. In this context substitution reactions are considered typical for an aromatic molecule and addition reactions and Diels Alder reactions are considered as typical olefine

Table 7. Comparison of experimental susceptibilities and susceptibilities calculated within the local model from the atomic increments listed in Table 6. $\chi_{\parallel} = (\chi_{aa} + \chi_{bb})/2$, $\chi_{\perp} = \chi_{cc}$, c-axis perpendicular to the plane of the ring. Isoprene at the top of the list was included as an example of an open chain molecule where generally $\chi_{\parallel}$ and $\chi_{\perp}$ are reproduced well within the local modell. The values of the susceptibilities are given in units of 10^{-6} erg/Gauss^{2}mole.

Molecule	Experimental susceptibilities $\chi_{\parallel}$ $\chi_{\perp}$	Nonlocal susceptibilities $\chi_{\parallel}$ $\chi_{\perp}$
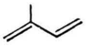	−35.7 [21] −52.8	1.6 − 0.3
	−33.3 [15] −67.5	− 1.1 −18.8
	−31.9 [22] −70.6	− 0.8 −25.3
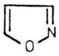	−25.6 [23] −62.8	− 0.5 −26.9
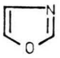	−24.4 [23] −65.1	0.7 −29.2
	−40.7 [22] −90.8	− 2.8 −39.1
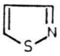	−33.6 −84.6	− 1.0 −38.1
	−32.8 −86.1	− 0.2 −39.6
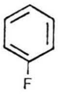	−38.8 [24] −97.2	− 1.5 −38.4

reactions. In this sense the replacement of a $\rangle$CH group by the isoelectronic $\rangle$N group leaves the chemical reactivity of the ring molecule essentially unchanged and in good correlation the value of $\chi_{\perp}{}^{\text{nonlocal}}$ remains constant too.

In an attempt to get a deeper understanding of $\chi_{\perp}{}^{\text{nonlocal}}$ we have also carried out CNDO calculations. Although the quality of the CNDO-approach may be questionable for molecules with highly delocalized orbitals it may be interesting to note that in each of the closely related pairs Thiazole/Isothiazole; Oxazole/Isoxazole and 1,2-Defluorobenzene/1,3-Difluorobenzene the partner with the less negative $\chi_{\perp}{}^{\text{nonlocal}}$ also turns out to be the one which shows the higher "CNDO-polarity" in the ring. By "CNDO-polarity" we mean the sum of the absolute values of the excess CNDO atomic charges of the ring atoms. In other words, the more the CNDO-calculation indicates that certain atoms tend to attract, others to give off electrons, the smaller is the value of the negative nonlocal susceptibility.

Acknowledgements

Wir danken Herrn Prof. Dr. H. Dreizler für die kritische Durchsicht des Manuskripts. Der Deutschen Forschungsgemeinschaft und dem Fonds der Chemie sei für die finanzielle Unterstützung gedankt. Die numerischen Rechnungen wurden im Rechenzentrum der Christian-Albrechts-Universität, Kiel, durchgeführt.

[1] E. Hückel, Z. Physik **70**, 204 (1931); **72**, 310 (1931); **76**, 628 (1932).

[2] J. Labarre and F. Crasnier, Fortschr. Chem. Forsch. **24**, 33 (1971).

[3] L. Pauling, J. Chem. Phys. **4**, 673 (1936). F. London, J. Phys. Radium **8**, 397 (1937).

[4] J. A. Pople, W. G. Schneider, and J. H. Bernstein, High-resolution Nuclear Magnetic Resonance, McGraw-Hill, London 1956. R. C. Haddon, V. R. Haddon, and L. M. Jackman, Fortschr. Chem. Forsch. **16**, 103 (1971).

[5a] Landolt-Börnstein: New Series, Group II: Atomic and Molecular Physics, Vol. 6. — b) D. H. Sutter and W. H. Flygare, Topics Curr. Chem. **63**, 89 (1976).

[6] R. C. Benson, Ph. D. Thesis, Dept. of Chemistry, Univ. of Illinois, Urbana Ill. 1972. — A. K. Burnham, Jaekeun Lee, T. G. Schmalz, P. Beak, and W. H. Flygare, J. Amer. Chem. Soc. **99**, 1836 (1977).

[7] D. H. Sutter, Z. Naturforsch. **26a**, 1644 (1971).

[8] L. Engelbrecht and D. H. Sutter, Z. Naturforsch. **31a**, 670 (1976). W. Gordy and R. L. Cook, Microwave Molecular Spectra Interscience Publ., J. Wiley, New York 1970, Section 9.4.

[9] The matrix elements used are given in the App. of K. F. Dössel, J. Wiese, and D. H. Sutter, Z. Naturforsch. **33a**, 21 (1978); compare also Ref. [5b], Chap. III,I.

[10] K.-F. Dössel and D. H. Sutter, Z. Naturforsch. **34a**, 469 (1979).

[11] Handbook of Chemistry and Physics, 56. Ed. CRC press, Cleveland, Ohio.

[12] L. N. Mulay, Techniques for Measuring Magnetic Susceptibilities, in Physical Methods of Chemistry, Part IV, Editor A. Weissberger, John Wiley Intersci. New York 1972.

[13] R. A. Flath, N. Henderson, and R. E. Lundi, Appl. Spectrosc. **21**, 183 (1967). K. Hatada, Y. Terawaki, and H. Okuda, Bull. Chem. Soc. Japan **42**, 1781 (1969). — W. Czieslik, Ph. D. Thesis, Univ. of Kiel 1976.

[14] P. Pascal, Ann. Chim. Physique **19**, 5 (1910), **25**, 289 (1912), **29**, 218 (1913).

[15] R. C. Benson and W. H. Flygare, J. Amer. Chem. Soc. **92**, 7523 (1970).

[16] A detailed description of the procedure is also given in Ref. [5b], Chapter II.C.

[17] T. G. Schmalz, C. L. Norris, and W. H. Flygare, J. Amer. Chem. Soc. **95**, 7961 (1973).

[18] A. Wardley, V. E. Williams, N. L. Owen, and J. Sheridan, Nature London **216**, 1301 (1967).
[19] L. Nygaard, E. Asmussen, J. H. Hog, R. L. Maheshwari, C. H. Nielsen, I. B. Petersen, J. Rastrup-Anderson, and G. O. Sørensen, J. Mol. Struct. 8, 225 (1971); **9**, 220 (1971).
[20] O. Stiefvater, Z. Naturforsch. **31a**, 1682 (1976).
[21] T. G. Schmalz, C. L. Norris, and W. H. Flygare, J. Amer. Chem. Soc. **95**, 7961 (1973).
[22] D. H. Sutter and W. H. Flygare, J. Amer. Chem. Soc. **91**, 4063 (1969).
[23] J. Davidson, A. K. Burnham, B. Siegel, and W. H. Flygare, J. Amer. Chem. Soc. **96**, 7394 (1974).
[24] W. Hüttner and W. H. Flygare, J. Chem. Phys. **50**, 2863 (1969).